Multidimensional, high precision beam spin asymmetry measurements of semi-inclusive pion production off the proton with CLAS12

S. Diehl[1,2⋆] for the CLAS collaboration

1 II. Physikalisches Institut der Universität Gießen, 35392 Gießen, Germany
2 University of Connecticut, Storrs, Connecticut 06269, USA

⋆ stefan.diehl@exp2.physik.uni-giessen.de

Proceedings for the XXVIII International Workshop on Deep-Inelastic Scattering and Related Subjects, Stony Brook University, New York, USA, 12-16 April 2021
doi:10.21468/SciPostPhysProc.8

Abstract

High precision measurements of the polarized electron beam-spin asymmetry in SIDIS from the proton have been performed using a 10.6 GeV incident electron beam and the CLAS12 spectrometer at Jefferson Lab. The proceeding reports a multidimensional study of the structure function ratio $F_{LU}^{\sin\phi}/F_{UU}$ extracted from single pion (π^+, π^-, π^0) SIDIS data over a large kinematic range in z, x_B, P_T and virtualities Q^2 ranging from 1 GeV^2 up to 7 GeV^2. $F_{LU}^{\sin\phi}$ is a twist-3 quantity that can reveal novel properties of quark-gluon correlations within the nucleon.

Received 10-07-2021
Accepted 17-03-2022
Published 14-07-2022
doi:10.21468/SciPostPhysProc.8.149

1 Introduction

Many decades of experiments in deep inelastic scattering (DIS) of lepton beams off nucleons have mapped out the momentum distributions of the partons in the nucleon in terms of one-dimensional parton distribution functions (PDFs) [1, 2]. While these measurements provided significant insight into the structure of the nucleon, many important and interesting aspects of the nucleon structure cannot be revealed in this one dimensional picture since PDFs are essentially averaged over all degrees of freedom except the longitudinal momentum. Therefore, they cannot address questions such as: Do quarks undergo orbital motion? Is there a connection between the motion of quarks, their spin and the spin of the proton? How is the total spin of the proton built up from the spin and the orbital angular momentum of partons? Today, the possibility of three-dimensional (3-D) imaging exists, which allows such questions to be addressed [3–5]. Remarkable theoretical advances over the past decade have led to a rigorous framework where information on the confined motion of the partons inside a fast moving nucleon is matched to transverse momentum dependent parton distribution functions (TMDs) [4,6]. In particular, TMDs can encode information about the orbital motion of quarks in the parent nucleon and correlations between the motion of partons and their spin. Semi-inclusive DIS (SIDIS), where a specified hadron is detected in the final state, is a powerful tool to study the transverse momentum dependent partonic structure of the nucleon. Spin asymmetries in polarized SIDIS can be related to TMDs and fragmentation functions (FFs). Since beam single spin asymmetries (SSAs) are subleading twist-3 objects, they are expected to be suppressed by $\mathcal{O}(M/Q)$, where M is the target mass and Q^2 is the photon virtuality. However, with the energies available at existing fixed-target facilities, contributions of the order $\mathcal{O}(M/Q)$ could be sizable, making such twist-3 contributions accessible and thereby providing access to the information they contain about quark-gluon correlations.

The diagram in Fig. 1(a) shows the SIDIS scattering process, including the involved TMDs and FFs, and Fig. 1(b) shows the definition of the reaction kinematics.

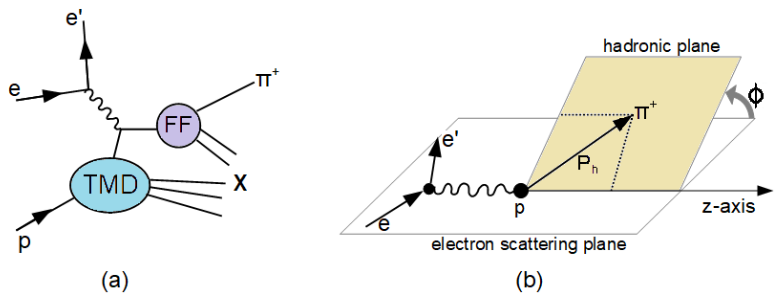

Figure 1: (a) Schematic diagram of the single pion semi-inclusive deep inelastic scattering process with the involved parton distributions and fragmentation functions. (b) Definition of the reaction kinematics of single pion SIDIS.

Beam SSAs are defined as:

$$SSA(z,P_T,\phi,x_B,Q^2)=\frac{d\sigma^+-d\sigma^-}{d\sigma^++d\sigma^-}=\frac{A_{LU}^{\sin\phi}\sin\phi}{1+A_{UU}^{\cos\phi}\cos\phi+A_{UU}^{\cos2\phi}\cos2\phi}, \tag{1}$$

where $d\sigma^\pm$ is the differential cross section for the two beam helicity states (±). The subscripts of the moments A_{ij} represent the longitudinally polarized (L) or unpolarized (U) state of the beam and the target. As defined in Fig. 1 (b), ϕ is the azimuthal angle between the electron scattering and the hadronic reaction plane.
The $\sin\phi$ moment $A_{LU}^{\sin\phi}$ is directly related to the polarized structure function $F_{LU}^{\sin\phi}$:

$$A_{LU}^{\sin\phi}=\frac{\sqrt{2\epsilon(1-\epsilon)}\,F_{LU}^{\sin\phi}}{F_{UU,T}+\epsilon F_{UU,L}}=\sqrt{2\epsilon(1-\epsilon)}\,\frac{F_{LU}^{\sin\phi}}{F_{UU}}, \tag{2}$$

where $F_{UU,T}$ and $F_{UU,L}$ represent the contributions from transversly and longitudinally polarized virtual photon, and ϵ is the ratio of their fluxes.

The structure function $F_{LU}^{\sin\phi}$, which is related to the quark-gluon-quark correlations in the proton can be expressed as a convolution ($\mathcal{C}$), of TMDs and FFs [4,7]:

$$F_{LU}^{\sin\phi}=\frac{2M}{Q}\,\mathcal{C}\left[-\frac{\hat{\mathbf{h}}\cdot\mathbf{k}_T}{M_h}\left(x_BeH_1^\perp+\frac{M_h}{M}f_1\frac{\tilde{G}^\perp}{z}\right)+\frac{\hat{\mathbf{h}}\cdot\mathbf{p}_T}{M}\left(x_Bg^\perp D_1+\frac{M_h}{M}h_1^\perp\frac{\tilde{E}}{z}\right)\right], \tag{3}$$

where e is a twist-3 PDF, $H_1^\perp$ is the Collins FF, f_1 is an unpolarized distribution function, $\tilde{G}^\perp$ is a twist-3 FF, $g^\perp$ is a twist-3 T-odd distribution function, D_1 is an unpolarized FF, $h_1^\perp$ is the

Boer-Mulders function and $\tilde{E}$ is a twist-3 FF [4,8]. Furthermore, M_h is the pion mass and $\hat{\mathbf{h}}$ is a unit vector in the direction of the pions transverse momentum, $\mathbf{p}_T$ and $\mathbf{k}_T$ are the intrinsic quark transverse momentum in the generic distribution functions f_1 and in the fragmentation function D_1 [4].

2 Experimental procedures

In this work, we extract the structure function ratio $F_{LU}^{\sin\phi}/F_{UU}$ in single pion SIDIS of longitudinally polarized electrons off unpolarized protons with a wide range of fully differential kinematics in the Q^2 range from 1.7 to 7.0 GeV^2, x_B from 0.13 - 0.52, z from 0.18 - 0.7 and P_T up to 0.85 GeV. Here we define the virtuality of the collision as Q^2, the fraction of the proton's momentum carried by the struck quark as x_B, the energy fraction of the virtual photon carried by the outgoing hadron as z and the transverse momentum of the final state hadron as P_T.

The measurements were performed at Jefferson Lab with CLAS12 (CEBAF Large Acceptance Spectrometer for experiments at 12 GeV) [9]. The incident electron beam was longitudinally polarized and had an energy of 10.6 GeV. The target was unpolarized liquid hydrogen. The CLAS12 forward detector consists of six identical sectors within a toroidal magnetic field. The momentum and the charge of the particles were determined by 3 regions of drift chambers. The electron identification was based on a lead-scintillator electromagnetic sampling calorimeter in combination with a Cherenkov counter, while positive pions were identified by time-of-flight measurements.

Deeply inelastic scattered electrons, were selected by cuts on $Q^2 > 1\,\text{GeV}^2$, and on the invariant mass of the hadronic final state $W > 2$ GeV. The energy fraction of the incoming lepton carried by the virtual photon y was limitted to < 0.75. In addition, to reduce the contribution from exclusive channels, the $e'\pi^+X$ missing mass was required to be larger than 1.5 GeV. For the multidimensional binning, first the electron variables are sorted in 9 bins in Q^2 and x_B (see Fig. 2). For each of these Q^2 - x_B bins a binning is applied to z and P_T as shown for the example of Q^2 - x_B bin 1 in Fig. 2. The kinematic distributions were found to be very similar for all 3 pions. Therefore the same binning scheme can be applied to π^+, π^- and π^0.

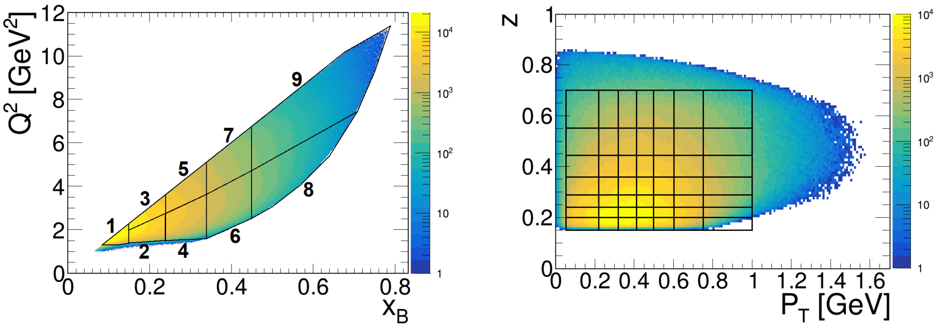

Figure 2: Left: Distribution of Q^2 versus x_B. The bin boundaries are shown as black lines and the bin numbering is given. Right: Correlation between z and P_T for Q^2 - x_B - bin 1. The black lines indicate the bin borders. [10]

The beam SSA and its statistical uncertainty were determined experimentally from the number of counts with positive and negative helicity ($N_i^{\pm}$) in a specific bin i as:

$$SSA = \frac{1}{P_e}\frac{N_i^+ - N_i^-}{N_i^+ + N_i^-}\ ,\ \sigma_{SSA} = \frac{1}{P_e}\sqrt{\frac{1-(P_e\,SSA)^2}{N_i^+ + N_i^-}}, \tag{4}$$

where $P_e = 86.3\% \pm 2.6\%$ is the average magnitude of the beam polarization. $A_{LU}^{\sin\phi}$ was extracted by a a fit of a $\sin\phi$ function to the ϕ dependence of the beam SSA. The obtained $A_{LU}^{\sin\phi}$ moment is then related to $F_{LU}^{\sin\phi}/F_{UU}$ via Eq. (2). Several sources of systematic uncertainty were investigated, including beam polarization, radiative effects, particle identification and contamination from baryon resonances and exclusive ρ meson production. A detailed Monte Carlo simulation was performed to study acceptance and bin-migration effects, which were both found to be negligible compared to the other contributions. The influence of additional azimuthal modulations $\cos\phi$ and $\cos 2\phi$ on the extracted $\sin\phi$ amplitude was also evaluated, and found to be negligible. More details can be found in [10].

3 Results

The structure function ratio $F_{LU}^{\sin\phi}/F_{UU}$ has been extracted for each of the obtained 344 bins. Figure 3 shows the z and P_T dependencies of π^+ for selected P_T and z bins in different bins of Q^2 and x_B (bin 1: $Q^2 = 1.71$ GeV^2, $x_B = 0.13$, bin 2: $Q^2 = 2.02$ GeV^2, $x_B = 0.19$, bin 7: $Q^2 = 4.89$ GeV^2, $x_B = 0.39$, bin 9: $Q^2 = 6.55$ GeV^2, $x_B = 0.52$).

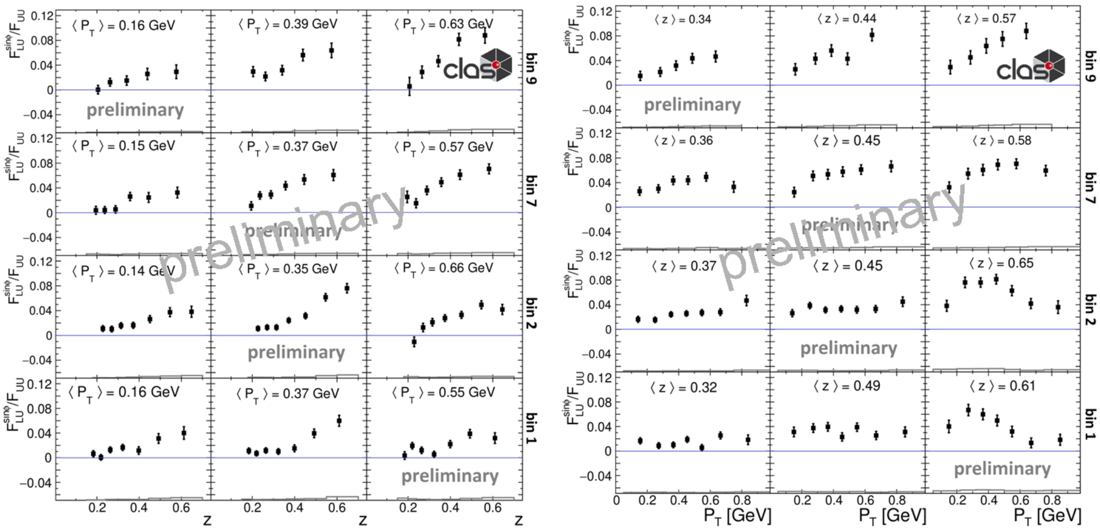

Figure 3: z dependence (left) and P_T dependence (right) of $F_{LU}^{\sin\phi}/F_{UU}$ for π^+ in increasing P_T / z bins (left to right) and for different Q^2-x_B bins. The systematic uncertainty is given by the histogram above the horizontal axes.

For π^+ it can be observed that the z dependence changes from a more flat behaviour at small P_T, Q^2, and x_B values to a steep increase at large P_T, Q^2, and x_B values. Also for the P_T dependence a small magnitude with a nearly flat behaviour can be observed at small Q^2, x_B, and z values, while for increasing z values a peaking structure with varying mean value and width can be observed at small Q^2 and x_B, while an increasing trend becomes dominant at large Q^2 and x_B values. Detailed comparisons to TMD based theoretical models are available for the case of π^+ in Ref. [10].

Preliminary results for the z and P_T dependence of π^0 and π^- are shown in Fig. 4. The same multidimensional bins as for π^+ in Fig. 3 are used. For π^0 a positive $F_{LU}^{\sin\phi}/F_{UU}$ value can be observed, which has a similar magnitude as for π^+. However some differences like a different trend and different structures of the P_T dependence in some bins can be identified.

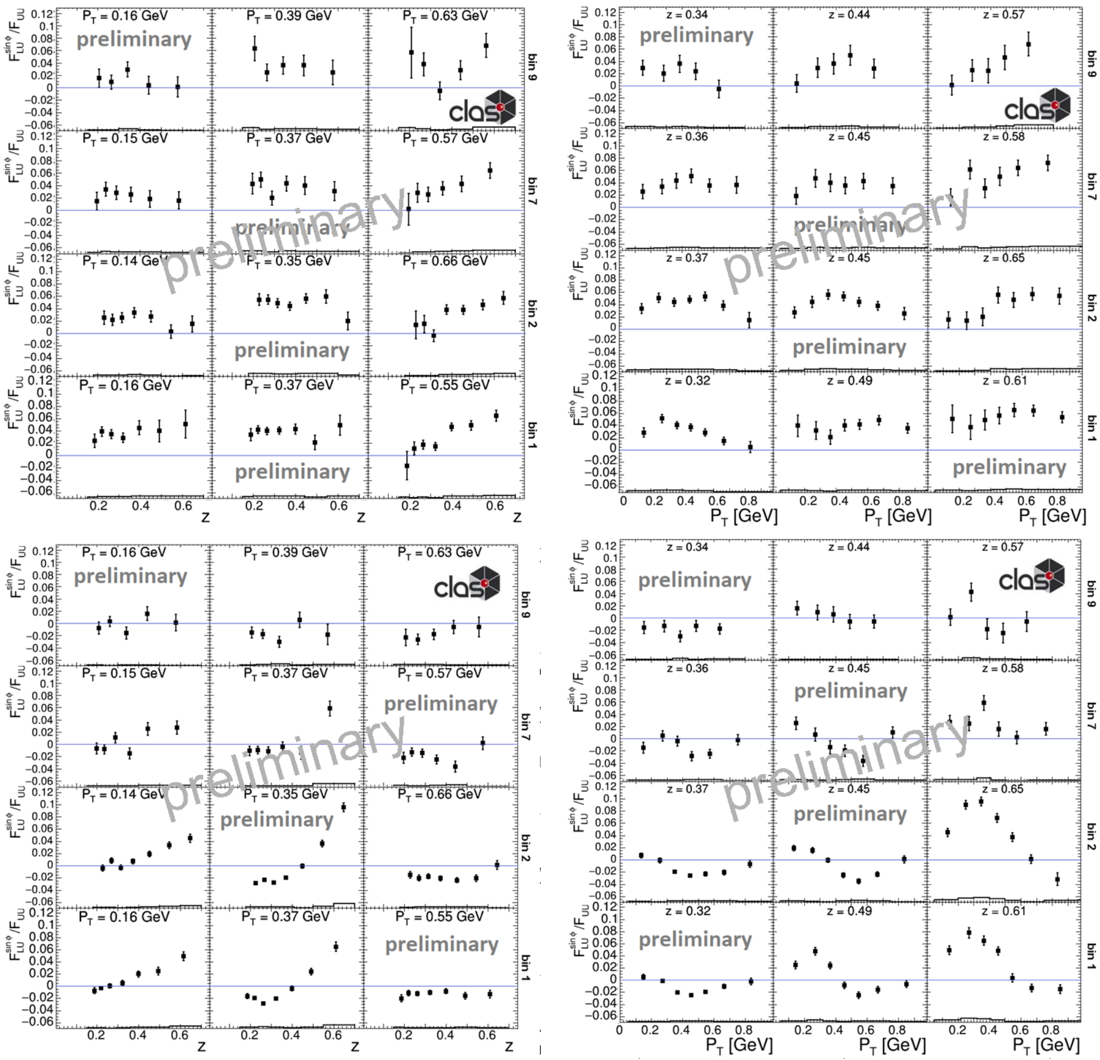

Figure 4: **Upper panels:** z dependence (left) and P_T dependence (right) of $F_{LU}^{\sin\phi}/F_{UU}$ for π^0 in different P_T / z and Q^2-x_B bins. **Lower panels:** z dependence (left) and P_T dependence (right) of $F_{LU}^{\sin\phi}/F_{UU}$ for π^- in different P_T / z and Q^2-x_B bins. A preliminary estimate of the systematic uncertainty is given by the histogram above the horizontal axes.

In contrast to this, $F_{LU}^{\sin\phi}/F_{UU}$ shows mostly negative values which are close to zero for π^- at high Q^2 and x_B values (bin 7 and 9). However at lower Q^2 and x_B values (bin 1 and 2) sign transition occur between small and large P_T values as well as between small and large z values. In the kinematic domain of large z and small P_T values, a positive magnitude of up to 0.1 is reached, while at small z and intermediate to large P_T negative values with a typical order of -0.02 are observed. For π^0 and π^- more detailed studies of the systematic uncertainty are still ongoing.

4 Conclusion

In summary, the structure function ratio $F_{LU}^{\sin\phi}/F_{UU}$ corresponding to the polarized electron beam single spin asymmetry in semi-inclusive deep inelastic scattering has been measured for all three pions over a wide range of kinematics in a fully multidimensional study. The fully differential study revealed structures, which were not visible in previous integrated studies like [11]. Including these multidimensional measurements into global fits, in combination with future measurements of unpolarized cross sections, as well as polarized target spin asymmetries, will provide new, strong constraints on the participating TMDs and FFs. The high precision of the fully multidimensional measurement, enables a detailed comparison to theoretical models for the first time. More details on this aspect can be found in Ref. [10]. More detailed comparisons for all three pions in contrast to theoretical models and the interpretation of the underlying physics effects will follow once the studies of the systematic uncertainty of π^0 and π^- are completed.

Acknowledgements

We acknowledge the outstanding efforts of the staff of the Accelerator and the Physics Divisions at Jefferson Lab in making this experiment possible.

Funding information This work was supported in part by the U.S. Department of Energy, the National Science Foundation (NSF), the Italian Istituto Nazionale di Fisica Nucleare (INFN), the French Centre National de la Recherche Scientifique (CNRS), the French Commissariat pour l′Energie Atomique, the UK Science and Technology Facilities Council, the National Research Foundation (NRF) of Korea, the Helmholtz-Forschungsakademie Hessen für FAIR (HFHF) and the Ministry of Science and Higher Education of the Russian Federation. The Southeastern Universities Research Association (SURA) operates the Thomas Jefferson National Accelerator Facility for the U.S. Department of Energy under Contract No. DE-AC05-06OR23177.

References

[1] J. Gao, L. Harland-Lang and J. Rojo, *The structure of the proton in the LHC precision era*, Phys. Rep. **742**, 1 (2018), doi:10.1016/j.physrep.2018.03.002.

[2] J. J. Ethier and E. R. Nocera, *Parton Distributions in Nucleons and Nuclei*, Annu. Rev. Nucl. Part. Sci. **70**, 43 (2020), doi:10.1146/annurev-nucl-011720-042725.

[3] K. Goeke, A. Metz and M. Schlegel, *Parameterization of the quark–quark correlator of a spin-$\frac{1}{2}$ hadron*, Phys. Lett. B **618**, 90 (2005). doi:10.1016/j.physletb.2005.05.037

[4] A. Bacchetta, M. Diehl, K. Goeke, A. Metz, P. J. Mulders and M. Schlegel, *Semi-inclusive deep inelastic scattering at small transverse momentum*, J. High Energy Phys. **02**, 093 (2007), doi:10.1088/1126-6708/2007/02/093.

[5] A. Metz and A. Vossen, *Parton fragmentation functions*, Prog. Part. Nucl. Phys. **91**, 136 (2016), doi:10.1016/j.ppnp.2016.08.003.

[6] B. Pasquini and S. Rodini, *The twist-three distribution $e(x,k_\perp)$ in a light-front model*, Phys. Lett. B **788**, 414 (2019), doi:10.1016/j.physletb.2018.11.033.

[7] J. Levelt and P. J. Mulders, *Time reversal odd fragmentation functions in semi-inclusive scattering of polarized leptons from unpolarized hadrons*, Phys. Lett. B **338**, 357 (1994), doi:10.1016/0370-2693(94)91391-9.

[8] M. Anselmino, A. Mukherjee and A. Vossen, *Transverse spin effects in hard semi-inclusive collisions*, Prog. Part. Nucl. Phys. **114**, 103806 (2020), doi:10.1016/j.ppnp.2020.103806.

[9] V. D. Burkert et al., *The CLAS12 Spectrometer at Jefferson Laboratory*, Nucl. Instr. Meth. Phys. Research Sec. A **959**, 163419 (2020), doi:10.1016/j.nima.2020.163419.

[10] S. Diehl et al., *Multidimensional, High Precision Measurements of Beam Single Spin Asymmetries in Semi-inclusive π^+ Electroproduction off Protons in the Valence Region*, Phys. Rev. Lett. **128**, 062005 (2022), doi:10.1103/PhysRevLett.128.062005.

[11] W. Gohn et al., *Beam-spin asymmetries from semi-inclusive pion electroproduction*, Phys. Rev. D **89**, 072011 (2014), doi:10.1103/PhysRevD.89.072011.